PROCEEDINGS OF SCIENCE

First results of pulsar observations with the LST-1

Álvaro Mas-Aguilar ,[a,*] Giulia Brunelli ,[b,c] Giovanni Ceribella ,[d] Marcos López-Moya [a] and Rubén López-Coto [c] for the CTA LST project

[a] *IPARCOS and Department of EMFTEL, Universidad Complutense de Madrid, E-28040, Madrid, Spain*
[b] *INAF-OAS and Università di Bologna, 40129, Bologna, Italy*
[c] *Instituto de Astrofísica de Andalucía-CSIC, Glorieta de la Astronomía s/n, 18008, Granada, Spain*
[d] *Max-Planck-Institut for Physics, 80805 Munich, Germany*
E-mail: alvmas@ucm.es, marcos@gae.ucm.es, rlopezcoto@iaa.es, giulia.brunelli6@studio.unibo.it, ceribell@mpp.mpg.de

After the discovery of Crab, Vela, and Geminga pulsars at Very High Energies, the search for new pulsars at tens of GeV has been gaining huge importance. However, their steep spectra along with the sensitivity of the current generation of Imaging Atmospheric Cherenkov telescopes (IACTs) are limiting the capability to detect more pulsars. The LST-1 is the first prototype of the Large-Sized Telescope of the forthcoming CTA observatory with enhanced sensitivity at tens of GeV. The LST-1 started its commissioning phase in 2018, and since then it has observed the Crab pulsar regularly. Here, we show the first results of the analysis of the Crab and other pulsars taken with the LST-1. The two characteristic emission peaks of the Crab pulsar, P1, and P2, are detected with high significance showing a clear improvement in sensitivity over the previous generation of IACTs. The spectrum is reconstructed up to 450 GeV for P1 and up to 700 GeV for P2. The low energy threshold of LST-1 also allows us to measure the spectrum of the Crab pulsar in the overlapping region with the Fermi-LAT and cross-calibrate both instruments. The results obtained with the first pulsar observations with the LST-1 confirm the excellent potential of LST telescopes to study and discover new pulsars in the near future.

38th International Cosmic Ray Conference (ICRC2023)
26 July - 3 August, 2023
Nagoya, Japan

*Speaker

© Copyright owned by the author(s) under the terms of the Creative Commons Attribution-NonCommercial-NoDerivatives 4.0 International License (CC BY-NC-ND 4.0).

PoS(ICRC2023)569

1. Introduction

Pulsars are highly magnetized neutron stars that show a very short period of rotation and emit radiation in the form of fast pulses. They were detected for the first time in the radio and, since then, many were found at other wavelengths. After the launch of Fermi-LAT in 2008, the number of pulsars confirmed at high energies (>100 MeV) increased from seven to more than one hundred in three years [1]. This supported the idea of pulsars as ubiquitous sources of GeV photons in the Galaxy, making these extreme objects ideal laboratories to probe particle acceleration mechanisms up to TeV energies. Most of the high-energy pulsars detected by Fermi-LAT exhibit Power Law (PL) spectra suppressed by an exponential cutoff at a few GeVs. As emission models in the inner magnetosphere generally predict steeper super-exponential cutoffs, an acceleration zone in the outer magnetosphere was recognized as the most probable mechanism to produce gamma-rays in pulsars. However, the detection with IACTs of three pulsars, Crab, Vela and Geminga, at a significance above 5σ hints to a PL extension beyond 50 GeV and even up to a few TeV [2]. This questions the classical models invoked to explain the gamma-ray production in these sources [3], which are now under debate.

The Very High Energy (VHE) emission of pulsars is concentrated at low energies due to its soft spectral indexes. Three of the brightest pulsars in the GeV range are currently detected by IACTs but the rest of the candidates are, in general, fainter. Therefore, the sensitivity of the current generation of IACTs is not enough to detect them and we need to rely on more sensitive instruments to obtain additional discoveries in the field. The Cherenkov Telescope Array will be the future gamma-ray observatory composed of tens of ground-based telescopes observing simultaneously [4]. It will be located in both the Southern and the Northern hemispheres and will combine telescopes of different sizes, each one optimized for a particular energy range, covering the entire VHE spectrum and aiming for a large variety of astronomical sources.

Among the different types of telescopes, the Large-Sized Telescopes (LSTs) are designed to operate at the lowest energies. Their large 23-metre diameter enables a reduction of the energy threshold down to a few tens of GeV. This results in a significant improvement of sensitivity with respect to the previous generation of IACTs for energies below 50 GeV, even when considering stereoscopic systems such as MAGIC's Sum-Trigger-II [6]. The LST-1 is the first prototype of its kind and was inaugurated in 2018 [5]. Since then, it has been in commissioning phase, including an extensive Crab Nebula and Pulsar observation campaign. Some first results of the performance of the LST-1 are reported in [7]. More recently, the LST-1 observed the Geminga pulsar already detected by the MAGIC telescopes [8]. The analysis of the first data of Crab and Geminga pulsars allowed us to characterize the potential of this telescope to detect new pulsars in the near future.

2. LST-1 observations of the Crab Pulsar

PSR J0534+220, also known as the Crab pulsar, is a young and energetic pulsar located at the center of the Crab Nebula. It shows a fast spin with a period of P$\approx$ 33 ms and $\dot{E} \approx 4.6 \cdot 10^{38}$erg s^{-1}. It was first detected in radio [9], and progressively observed at higher energies. It was discovered at VHEs by MAGIC [10] and VERITAS [11], and it has been an object of study in the following years

PoS(ICRC2023)569

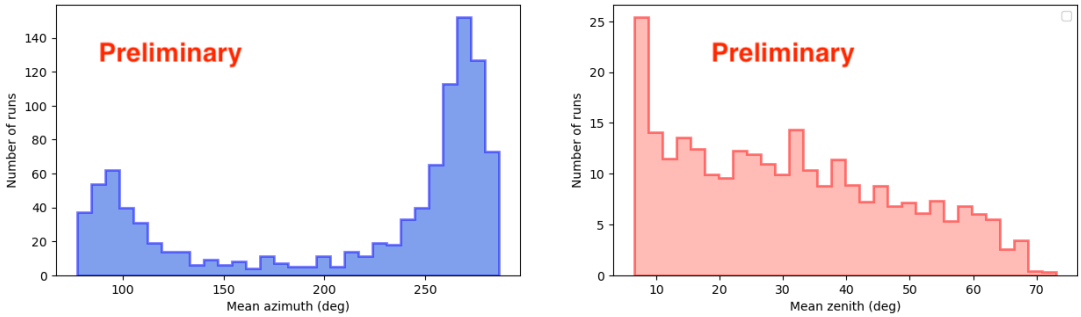

Figure 1: Distribution of azimuth and cosine of zenith angle of the LST-1 observations of the Crab Pulsar.

[12–14]. Its emission was detected up to the TeV range by the MAGIC telescopes [2], challenging the proposed models of emission. It is thus a perfect candidate to study the VHE pulsar emission.

The LST-1 observed the Crab pulsar from September 2020 to January 2023 and collected a total of 103 hours at zenith angle (Zd) below 50 degrees. From those, 76 hours were taken below 35 degrees with an energy threshold lower than 30 GeV. The distribution of the cosine of the Zd of the observations is depicted in Fig.1, peaking at Zd $<$ 15 degrees.

3. LST-1 analysis of the Crab Pulsar

To analyze the data a dedicated Montecarlo (MC) simulation was produced using the python package *lstmcpipe* [15]. These MC data were created with a spectral index of Γ=-2 and simulated on a declination of ~22.76 degrees, very near to the one of the Crab Nebula. They were also tuned to show a Night Sky Background (NSB) similar to the real one, estimated from the observations (see [7] for more details). These MC data were used to train dedicated Random Forest algorithms (RF) with some source-dependent parameters that depend on the real position of the source to enhance the performance at low energies.

For the DL1 to DL3 analysis of the data, we used the standard software for the LST-1 analysis `cta-lstchain` [16]. After the calibration and cleaning of the shower images in the camera, the RF were applied to the images so the reconstructed energy and incoming direction of the original particle can be estimated. An additional parameter called *Gammaness* describes also how probable is that the shower originated by a real gamma particle (*Gammaness*=1) or a hadron (*Gammaness*=0).

To remove the hadronic background some cuts were applied to the data. A cut on intensity above 80 photoelectrons was made for the data collected before August 2021, and a softer cut of 50 photoelectrons for data taken afterwards. The different cuts are due to different trigger thresholds before and after that date. Energy-dependent cuts on the angular direction (angle between the direction of the major axis of the shower image and the direction from the center of gravity of the ellipse to the source position) and *Gammaness* were also applied. Those cuts were computed using the 70% quantile of the MC distribution of the parameters. To compute the observed flux, the instrument response functions of the telescope (IRFs) need to be derived. Several IRFs were produced in different sky positions using particular test MC along the declination line. Therefore, the data were convoluted using the nearest IRF node in the sky position, and the dependence of the response with the zenith angle was taken into consideration.

PoS(ICRC2023)569

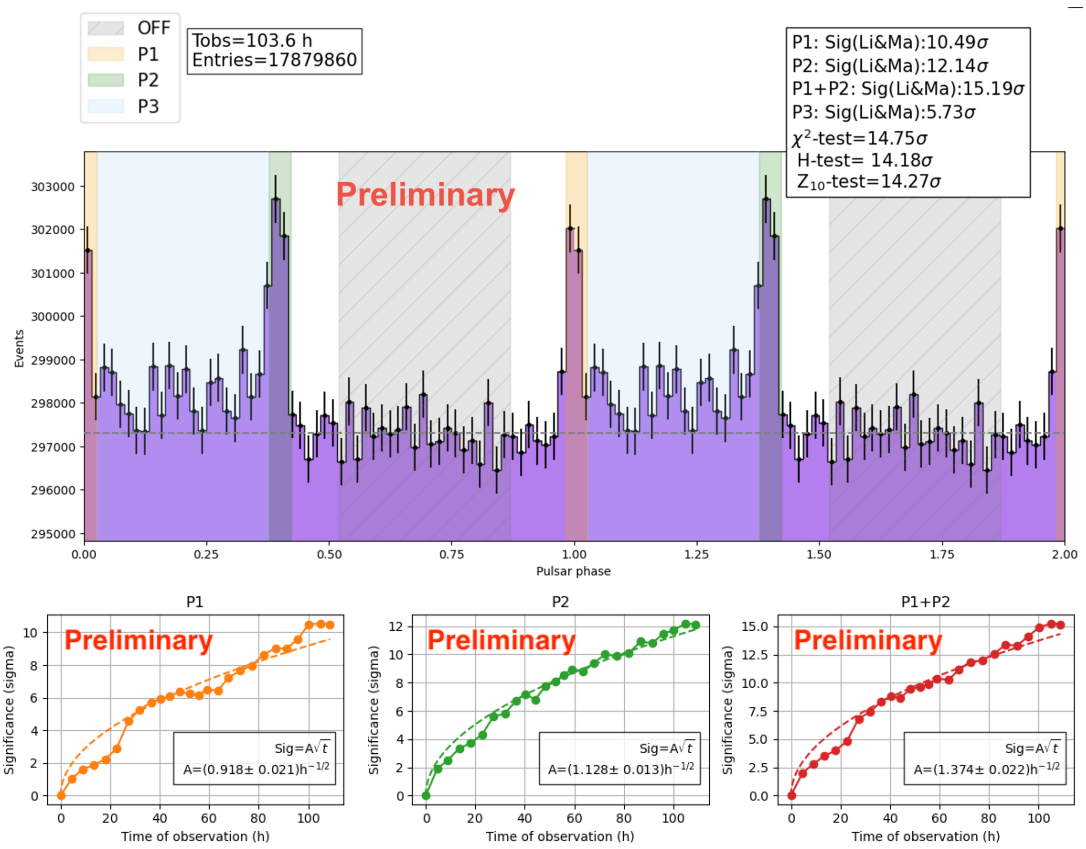

Figure 2: Phaseogram of the Crab Pulsar detected by LST-1. The two peaks are detected above 10 σ and the bridge emission is also significantly detected. The time evolution of the significance is plotted in the lower panels.

Finally, to analyze the pulsar, we used the arrival time of each event to interpolate the phase of the rotation of the star in which they were emitted. To achieve that, the publicly-available ephemeris provided by the Jodrell Bank observatory (http://www.jb.man.ac.uk/~pulsar/crab.html) [17] were employed to model the rotation of the star. This interpolation was performed using the PINT software package [18] for the pulsar analysis.

4. Phaseogram of the Crab Pulsar

The phaseogram of the Crab Pulsar from the observations performed at Zd $<$ 50 degrees is shown in Fig.2. The two well-known peaks of the pulsar are detected with the LST-1, both of them at a statistical significance above 10 σ. We followed the same definitions as previous results from MAGIC [2]: P1= [-0.017, 0.026] and P2= [0.377, 0.422]. The high significance of the softer P1 emission, at a similar level to the P2, confirms the low energy threshold of the telescope and its great performance at low energies. The bridge emission, roughly estimated as the emission between both peaks, is almost detected at 6 σ.

In the same plot, the evolution of the significance with the time of observations is plotted. The smooth distributions are fitted to the expected functions. The figure of merit is $\sigma/\sqrt{T_{\rm obs}}$ =

PoS(ICRC2023)569

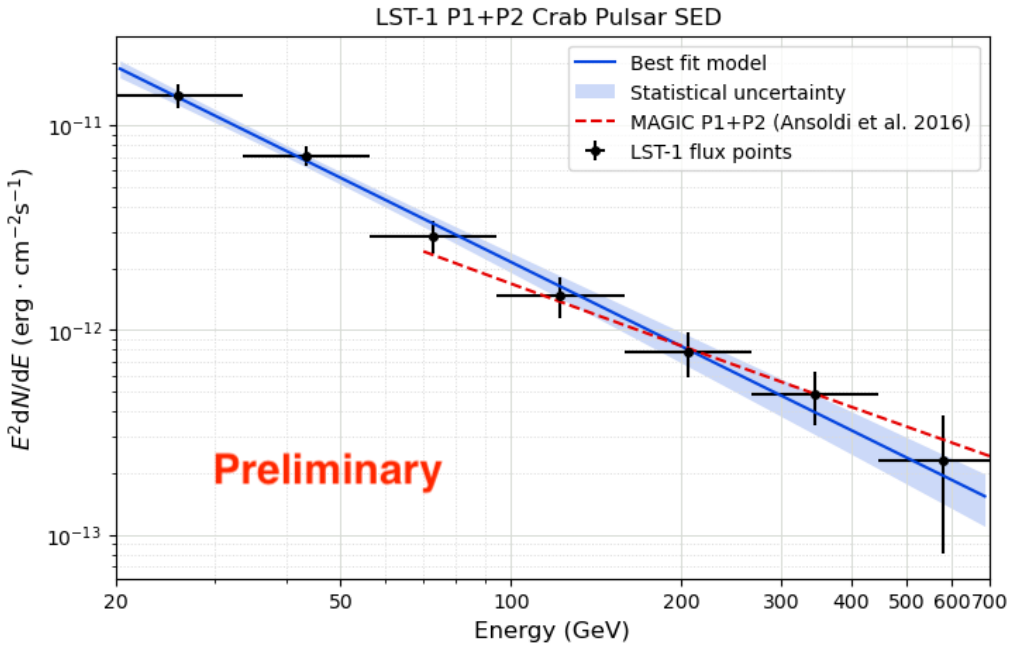

Figure 3: Spectral Energy Distribution (SED) of the overall pulsed emission (P1+P2) of the Crab Pulsar detected by the LST-1. The LST-1 flux points (in black) are represented together with the MAGIC flux (in red). The MAGIC flux was obtained by summing the best-fit models of P1 and P2 described in [2].

$(0.92 \pm 0.02)\ h^{-1/2}$ and $\sigma/\sqrt{T_{\rm obs}} = (1.13 \pm 0.01)\ h^{-1/2}$ for P1 and P2 respectively. Those numbers indicate an excellent performance of the telescope in mono observations, comparable to that obtained in stereoscopic observations by the two MAGIC telescopes [19], once the different zenith angle thresholds of each analysis are taken into consideration.

5. LST-1 Crab Pulsar SED

The SED of each peak was computed using a forward-folding likelihood method with *Gammapy* [20]. The results for the total pulsed emission are shown in Fig.3. It can be described by a PL with a spectral index of -3.37 ± 0.10. The PL extension beyond 500 GeVs confirms the results found by previous studies from MAGIC [2]. The individual SED for each peak can also be described by PL models that can be extended up to 450 GeV for P1 and 700 GeV for P2. The spectral indexes obtained are -3.69 ± 0.19 and -3.16 ± 0.10 for P1 and P2 respectively. Hence, the P1 SED decreases much faster than the P2 spectrum, and both cross at E~30 GeV. The spectral indexes found indicate a steeper spectrum than the ones reported in [14] and more similar to the Fermi-LAT + MAGIC results shown in [2]. This may indicate a smooth transition between LST-1 and Fermi-LAT.

Given the steep nature of the pulsar spectra, we performed a detailed study of the systematic uncertainties and repeated the analysis with different parameters to constrain their impact. Particularly, some of the energy-dependent cuts were changed to see the effect on the SED. A shift in the true energy of the MC was also introduced to study the effect of a systematic error in the energy reconstruction. Lastly, the results obtained using different versions of the analysis software and different subsamples of the data were compared. The maximum effect on the spectral indexes is

PoS(ICRC2023)569

found to be ∼ 10% for P1 and ∼ 5% for P2, mostly associated with the selection of the cuts used to remove the hadronic background.

6. Fermi-LAT and LST-1 joint-fit and cross-calibration

With the aim of studying the overall high energy emission of the Crab Pulsar, a new analysis of Fermi-LAT data using ∼13 years was done. We also performed some joint-fits to the LST-1 and Fermi-LAT data at E>100 MeV for both P1 and P2, using two models: a PL model suppressed with a sub-exponential cutoff ($dN/dE = f_0 \, (E/E_0)^{-\alpha} \exp\left(-(\lambda E)^{\beta}\right)$), and a smoothly-broken PL model ($dN/dE = f_0 \, (E/E_0) \left(1 + (E/E_b)^{\frac{\alpha_2-\alpha_1}{\gamma}}\right)^{-\gamma}$). All the fits converge successfully. Still, the sub-exponential cutoff one shows a higher deviation with respect to the flux points at E>100 GeV. The statistical results suggest that the smoothly-broken PL shows a better agreement with the experimental data for both, P1 and P2. This confirms a smooth transition between both instruments and reaffirms the PL extension at VHE found with the single LST-1 analysis.

Additionally, a systematic error in the reconstruction of the energy between Fermi-LAT and LST-1 was estimated. The joint fit was systematically repeated after multiplying the reconstructed energy of Fermi-LAT flux points by a factor that varied from 0.9 to 1.1. This way, a systematic error in the energy reconstruction of the Fermi-LAT flux points was introduced. The χ^2 statistic was computed for each fit to find the minimum among them. The χ^2 increased evenly as we used higher or lower factors, being the minimum at <3% for P1 and P2. Hence, the systematic error in the energy reconstruction between these instruments should be low enough to perform joint studies.

7. LST-1 observations and analysis of the Geminga Pulsar

PSR J0633+1746, or Geminga, is a classical example of a radio-quiet middle-aged gamma-ray pulsar. It has been known to be a gamma-ray emitter since 1972 [21] but, due to the absence of a radio-pulsed emission, it was not classified as a pulsar until 1992, when combined results in the gamma-ray [22] and soft X-ray [23] bands led to the discovery of pulsed emission with a period of P=237 ms. A surprising result on Geminga came in 2020 with the detection of pulsed emission above 15 GeV by the MAGIC Collaboration [8] since it was not thought that a middle-aged pulsar could reach such high energies. As for the Crab Pulsar, the MAGIC results suggested that the observed emission cannot be easily explained with the usual outer-gap pulsar emission models.

Geminga was also the second VHE pulsar detected by the LST-1. It was observed from December 2022 to March 2023, accumulating a total of 21 hours below Zd < 25 deg. For the analysis of the data sample, we adopted a source-dependent approach similar to the one for the Crab Pulsar. The same MC production simulated at declination ∼22.76° and with tuned NSB was used to train the RF models, and then the standard `cta-lstchain` software was used for the data reduction chain from DL1 to DL3. We applied a 50 p.e. cut in intensity and energy-dependent cuts on the *Gammaness* and angular direction based on the 70% quantile of the MC parameter distribution. Also in this case, the dependence of the response of the instrument with the zenith angle was taken into account for the IRF production. We used Fermi-LAT data to construct a timing solution for the Geminga pulsar and applied it to the LST-1 data[1].

[1]The Geminga ephemeris is available at https://www.mpp.mpg.de/~ceribell/geminga/index.php

PoS(ICRC2023)569

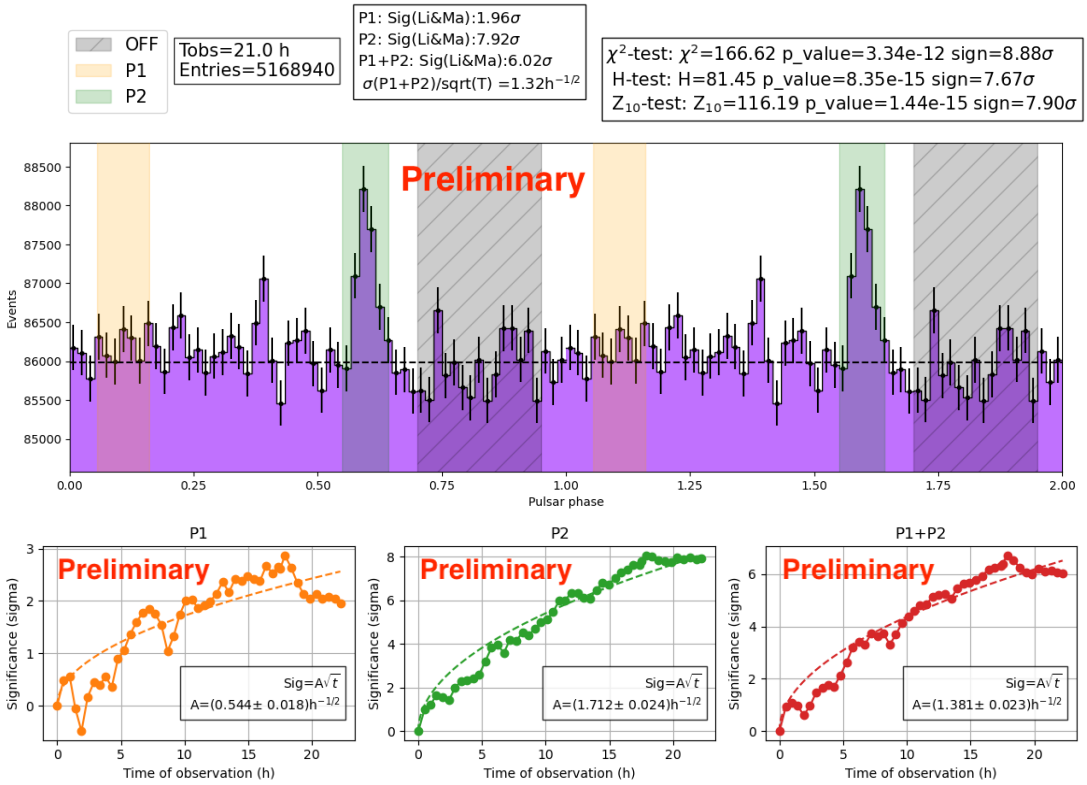

Figure 4: Phaseogram of the Geminga Pulsar detected by LST-1. P2 is detected at a statistical significance of 8σ, while P1 is below the 5σ threshold for detection. In the bottom plot, the time evolution of the significance is reported.

8. Phaseogram of the Geminga Pulsar

The phaseogram of the Geminga Pulsar obtained for the observations at Zd < 25 deg is shown in Fig.4. In accordance with those used by MAGIC [8], the definition of the phase region for the first peak is P1=[0.056, 0.16], while for the second peak it is P2=[0.550, 0.642]. P2 has been detected with a significance of about 8σ, while the signal from P1 only reaches a significance of about 2σ.

The bottom part of Fig.4 shows the evolution of the significance in time for P1, P2, and for both of them together, along with the respective fit functions. The figure of merit for P1 is $\sigma/\sqrt{T_{\rm obs}} = (0.54 \pm 0.02)\ h^{-1/2}$, while for P2 it is $\sigma/\sqrt{T_{\rm obs}} = (1.71 \pm 0.02)\ h^{-1/2}$. These results, even if preliminary, provide further evidence of the outstanding performance of LST-1 at the lowest energies: with only one telescope and around 20 hours of observations, the significance of both peaks was higher than the one obtained by MAGIC, which consists of two telescopes and observed Geminga for a total of 80 hours of good-quality data.

The trend for P1 is not as smooth as for P2 and this is mainly due to the influence of the mean zenith angle of some observations. However, on average, the P1 trend is increasing and, with future observations, LST-1 may be able to detect P1 for the first time with an IACT.

PoS(ICRC2023)569

Acknowledgments

This work was conducted in the context of the CTA LST project. We gratefully acknowledge financial support from the agencies and organizations listed here: https://www.lst1.iac.es/acknowledgements.html

References

[1] Abdo, A. A. et al., 2013, ApJS, 208, 17

[2] Abdo, A. A. et al., A&A, 585 (2016) A133

[3] Hirotani, K. , ApJ Letters, 688, 2008, 25-28

[4] Zanin, R. et al., PoS, 2021, ICRC2021, 005

[5] Mazin, D. et a.l, PoS 2021, ICRC2021, 872

[6] F. Dazzi et al., 2021, IEEE Transactions on Nuclear Science, 68, 7, 1473-1486

[7] CTA-LST Project et al. 2023, arXiv, 2306.12960

[8] MAGIC Collaboration, A&A, 643, 2020

[9] Lovelace, R. V. E. et al., IAU Circ., 1968, No. 2113, 1

[10] Aliu, E. et al., Science, 2008, 322, 5905, 1221

[11] Aliu, E. et al., Science, 2011, 334, 6052, 69-72

[12] Aleksić, J.et al., A&A, 2012, 540, A69

[13] Aleksić, J.et al., The American Astronomical Society, 742, 1, 43

[14] Aleksić, J.et al., A&A, 2014, 565, L12

[15] Garcia E. et al., 2022, arXiv, eprint: 2212.00120

[16] López-Coto, R. et al., ADASS XXX, ASP Conference Series, 532

[17] Lyne, A. G., Pritchard, R. S. and Graham-Smith, F. 1993. MNRAS, 265, 1003

[18] Luo, J. and Ransom, S. et al., The Astrophysical Journal, 2021, 911, 1, 45

[19] Ceribella, G. et al., PoS 2019, ICRC2019, 645

[20] Deil, C. and Lefaucheur, J. et al., PoS 2017, ICRC2017, 766

[21] Fichtel, C. E. et al., ApJ, 198, 1975, 163-182

[22] Bertsch, D. et al., Nature, 357, 1992, 306-307

[23] Halpern, J. and Holt, S., Nature, 357, 1992, 222–224

PoS(ICRC2023)569

Full Authors List: CTA LST Project

K. Abe[1], S. Abe[2], A. Aguasca-Cabot[3], I. Agudo[4], N. Alvarez Crespo[5], L. A. Antonelli[6], C. Aramo[7], A. Arbet-Engels[8], C. Arcaro[9], M. Artero[10], K. Asano[2], P. Aubert[11], A. Baktash[12], A. Bamba[13], A. Baquero Larriva[5,14], L. Baroncelli[15], U. Barres de Almeida[16], J. A. Barrio[5], I. Batkovic[9], J. Baxter[2], J. Becerra González[17], E. Bernardini[9], M. I. Bernardos[4], J. Bernete Medrano[18], A. Berti[8], P. Bhattacharjee[11], N. Biederbeck[19], C. Bigongiari[6], E. Bissaldi[20], O. Blanch[10], G. Bonnoli[21], P. Bordas[3], A. Bulgarelli[15], I. Burelli[22], L. Burmistrov[23], M. Buscemi[24], M. Cardillo[25], S. Caroff[11], A. Carosi[6], M. S. Carrasco[26], F. Cassol[26], D. Cauz[22], D. Cerasole[27], G. Ceribella[8], Y. Chai[8], K. Cheng[2], A. Chiavassa[28], M. Chikawa[2], L. Chytka[29], A. Cifuentes[18], J. L. Contreras[5], J. Cortina[18], H. Costantini[26], M. Dalchenko[23], F. Dazzi[6], A. De Angelis[9], M. de Bony de Lavergne[11], B. De Lotto[22], M. De Lucia[7], R. de Menezes[28], L. Del Peral[30], G. Deleglise[11], C. Delgado[18], J. Delgado Mengual[31], D. della Volpe[23], M. Dellaiera[11], A. Di Piano[15], F. Di Pierro[28], A. Di Pilato[23], R. Di Tria[27], L. Di Venere[27], C. Díaz[18], R. M. Dominik[19], D. Dominis Prester[32], A. Donini[6], D. Dorner[33], M. Doro[9], L. Eisenberger[33], D. Elsässer[19], G. Emery[26], J. Escudero[4], V. Fallah Ramazani[34], G. Ferrara[24], F. Ferrarotto[35], A. Fiasson[11,36], L. Foffano[25], L. Freixas Coromina[18], S. Fröse[19], S. Fukami[2], Y. Fukazawa[37], E. Garcia[11], R. Garcia López[17], C. Gasbarra[38], D. Gasparrini[38], D. Geyer[19], J. Giesbrecht Paiva[16], N. Giglietto[20], F. Giordano[27], P. Gliwny[39], N. Godinovic[40], R. Grau[10], J. Green[8], D. Green[8], S. Gunji[41], P. Günther[33], J. Hackfeld[34], D. Hadasch[2], A. Hahn[8], K. Hashiyama[2], T. Hassan[18], K. Hayashi[2], L. Heckmann[8], M. Heller[23], J. Herrera Llorente[17], K. Hirotani[2], D. Hoffmann[26], D. Horns[12], J. Houles[26], M. Hrabovsky[29], D. Hrupec[42], D. Hui[2], M. Hütten[2], M. Iarlori[43], R. Imazawa[37], T. Inada[2], Y. Inome[2], K. Ioka[44], M. Iori[35], K. Ishio[39], I. Jimenez Martinez[18], J. Jurysek[45], M. Kagaya[2], V. Karas[46], H. Katagiri[47], J. Kataoka[48], D. Kerszberg[10], Y. Kobayashi[2], K. Kohri[49], A. Kong[2], H. Kubo[2], J. Kushida[1], M. Lainez[5], G. Lamanna[11], A. Lamastra[6], T. Le Flour[11], M. Linhoff[19], F. Longo[50], R. López-Coto[4], A. López-Oramas[17], S. Loporchio[27], A. Lorini[51], J. Lozano Bahilo[30], P. L. Luque-Escamilla[52], P. Majumdar[53,2], M. Makariev[54], D. Mandat[45], M. Manganaro[32], G. Manicò[24], K. Mannheim[33], M. Mariotti[9], P. Marquez[10], G. Marsella[24,55], J. Martí[52], O. Martinez[56], G. Martínez[18], M. Martínez[10], A. Mas-Aguilar[5], G. Maurin[11], D. Mazin[2,8], E. Mestre Guillen[52], S. Micanovic[32], D. Miceli[9], T. Miener[5], J. M. Miranda[56], R. Mirzoyan[8], T. Mizuno[57], M. Molero Gonzalez[17], E. Molina[3], T. Montaruli[23], I. Monteiro[11], A. Moralejo[10], D. Morcuende[5], A. Morselli[38], V. Moya[5], H. Muraishi[58], K. Murase[2], S. Nagataki[59], T. Nakamori[41], A. Neronov[60], L. Nickel[19], M. Nievas Rosillo[17], K. Nishijima[1], K. Noda[2], D. Nosek[61], S. Nozaki[8], M. Ohishi[2], Y. Ohtani[2], T. Oka[62], A. Okumura[63,64], R. Orito[65], J. Otero-Santos[17], M. Palatiello[22], D. Paneque[8], F. R. Pantaleo[20], R. Paoletti[51], J. M. Paredes[3], M. Pech[45,29], M. Pecimotika[32], M. Peresano[28], F. Pfeiffle[33], E. Pietropaolo[66], G. Pirola[8], C. Plard[11], F. Podobnik[51], V. Poireau[11], M. Polo[18], E. Pons[11], E. Prandini[9], J. Prast[11], G. Principe[50], C. Priyadarshi[10], M. Prouza[45], R. Rando[9], W. Rhode[19], M. Ribó[3], C. Righi[21], V. Rizi[66], G. Rodriguez Fernandez[38], M. D. Rodríguez Frías[30], T. Saito[2], S. Sakurai[2], D. A. Sanchez[11], T. Šarić[40], Y. Sato[67], F. G. Saturni[6], V. Savchenko[60], B. Schleicher[33], F. Schmuckermaier[8], J. L. Schubert[19], F. Schussler[68], T. Schweizer[8], M. Seglar Arroyo[11], T. Siegert[33], R. Silvia[27], J. Sitarek[39], V. Sliusar[69], A. Spolon[9], J. Strišković[42], M. Strzys[2], Y. Suda[37], H. Tajima[63], M. Takahashi[63], H. Takahashi[37], J. Takata[2], R. Takeishi[2], P. H. T. Tam[2], S. J. Tanaka[67], D. Tateishi[70], P. Temnikov[54], Y. Terada[70], K. Terauchi[62], T. Terzic[32], M. Teshima[8,2], M. Tluczykont[12], F. Tokanai[41], D. F. Torres[71], P. Travnicek[45], S. Truzzi[51], A. Tutone[6], M. Vacula[29], P. Vallania[28], J. van Scherpenberg[8], M. Vázquez Acosta[17], I. Viale[9], A. Vigliano[22], C. F. Vigorito[28,72], V. Vitale[38], G. Voutsinas[23], I. Vovk[2], T. Vuillaume[11], R. Walter[69], Z. Wei[71], M. Will[8], T. Yamamoto[73], R. Yamazaki[67], T. Yoshida[47], T. Yoshikoshi[2], N. Zywucka[39]

[1]Department of Physics, Tokai University. [2]Institute for Cosmic Ray Research, University of Tokyo. [3]Departament de Física Quàntica i Astrofísica, Institut de Ciències del Cosmos, Universitat de Barcelona, IEEC-UB. [4]Instituto de Astrofísica de Andalucía-CSIC. [5]EMFTEL department and IPARCOS, Universidad Complutense de Madrid. [6]INAF - Osservatorio Astronomico di Roma. [7]INFN Sezione di Napoli. [8]Max-Planck-Institut für Physik. [9]INFN Sezione di Padova and Università degli Studi di Padova. [10]Institut de Fisica d'Altes Energies (IFAE), The Barcelona Institute of Science and Technology. [11]LAPP, Univ. Grenoble Alpes, Univ. Savoie Mont Blanc, CNRS-IN2P3, Annecy. [12]Universität Hamburg, Institut für Experimentalphysik. [13]Graduate School of Science, University of Tokyo. [14]Universidad del Azuay. [15]INAF - Osservatorio di Astrofisica e Scienza dello spazio di Bologna. [16]Centro Brasileiro de Pesquisas Físicas. [17]Instituto de Astrofísica de Canarias and Departamento de Astrofísica, Universidad de La Laguna. [18]CIEMAT. [19]Department of Physics, TU Dortmund University. [20]INFN Sezione di Bari and Politecnico di Bari. [21]INAF - Osservatorio Astronomico di Brera. [22]INFN Sezione di Trieste and Università degli Studi di Udine. [23]University of Geneva - Département de physique nucléaire et corpusculaire. [24]INFN Sezione di Catania. [25]INAF - Istituto di Astrofisica e Planetologia Spaziali (IAPS). [26]Aix Marseille Univ, CNRS/IN2P3, CPPM. [27]INFN Sezione di Bari and Università di Bari. [28]INFN Sezione di Torino. [29]Palacky University Olomouc, Faculty of Science. [30]University of Alcalá UAH. [31]Port d'Informació Científica. [32]University of Rijeka, Department of Physics. [33]Institute for Theoretical Physics and Astrophysics, Universität Würzburg. [34]Institut für Theoretische Physik, Lehrstuhl IV: Plasma-Astroteilchenphysik, Ruhr-Universität Bochum. [35]INFN Sezione di Roma La Sapienza. [36]ILANCE, CNRS . [37]Physics Program, Graduate School of Advanced Science and Engineering, Hiroshima University. [38]INFN Sezione di Roma Tor Vergata. [39]Faculty of Physics and Applied Informatics, University of Lodz. [40]University of Split, FESB. [41]Department of Physics, Yamagata University. [42]Josip Juraj Strossmayer University of Osijek, Department of Physics. [43]INFN Dipartimento di Scienze Fisiche e Chimiche - Università degli Studi dell'Aquila and Gran Sasso Science Institute. [44]Yukawa Institute for Theoretical Physics, Kyoto University. [45]FZU - Institute of Physics of the Czech Academy of Sciences. [46]Astronomical Institute of the Czech Academy of Sciences. [47]Faculty of Science, Ibaraki University. [48]Faculty of Science and Engineering, Waseda University. [49]Institute of Particle and Nuclear Studies, KEK (High Energy Accelerator Research Organization). [50]INFN Sezione di Trieste and Università degli Studi di Trieste. [51]INFN and Università degli Studi di Siena, Dipartimento di Scienze Fisiche, della Terra e dell'Ambiente (DSFTA). [52]Escuela Politécnica Superior de Jaén, Universidad de Jaén. [53]Saha Institute of Nuclear Physics. [54]Institute for Nuclear Research and Nuclear Energy, Bulgarian Academy of Sciences. [55]Dipartimento di Fisica e Chimica 'E. Segrè' Università degli Studi di Palermo. [56]Grupo de Electronica, Universidad Complutense de Madrid. [57]Hiroshima Astrophysical Science Center, Hiroshima University. [58]School of Allied Health Sciences, Kitasato University. [59]RIKEN, Institute of Physical and Chemical Research. [60]Laboratory for High Energy Physics, École Polytechnique Fédérale. [61]Charles University, Institute of Particle and Nuclear Physics. [62]Division of Physics and Astronomy, Graduate School of Science, Kyoto University. [63]Institute for Space-Earth Environmental Research, Nagoya University. [64]Kobayashi-Maskawa Institute (KMI) for the Origin of Particles and the Universe, Nagoya University. [65]Graduate School of Technology, Industrial and Social Sciences, Tokushima University. [66]INFN Dipartimento di Scienze Fisiche e Chimiche - Università degli Studi dell'Aquila and Gran Sasso Science Institute. [67]Department of Physical Sciences, Aoyama Gakuin University. [68]IRFU, CEA, Université Paris-Saclay. [69]Department of Astronomy, University of Geneva. [70]Graduate School of Science and Engineering, Saitama University. [71]Institute of Space Sciences (ICE-CSIC), and Institut d'Estudis Espacials de Catalunya (IEEC), and Institució Catalana de Recerca I Estudis Avançats (ICREA). [72]Dipartimento di Fisica - Universitá degli Studi di Torino. [73]Department of Physics, Konan University.

PoS(ICRC2023)569